Peertechz Journal of Biomedical Engineering

Yu-Hsiang Lee[1,2,3]* and Yun-Han Lai[1]

[1]Graduate Institute of Biomedical Engineering, National Central University, Taoyuan City, Taiwan
[2]Department of Biomedical Sciences and Engineering, National Central University, Taoyuan City, Taiwan
[3]Department of Chemical and Materials Engineering, National Central University, Taoyuan City, Taiwan

Dates: **Received:** 25 August, 2015; **Accepted:** 25 September, 2015; **Published:** 28 September, 2015

***Corresponding author:** Yu-Hsiang Lee, Department of Biomedical Sciences and Engineering, National Central University. No. 300, Jhongda Rd., Taoyuan City, 32001, Taiwan R.O.C. Tel: (+886)-3-422-7151; Ext #: 37352; Fax: (+886)-3-280-4627; E-mail: yuhsianl@ncu.edu.tw

www.peertechz.com

Keywords: Indocyanine green; PLGA nanoparticle; PEG; anti-HER2 antibody; Near Infrared; Phototherapy

Research Article

Fabrication and Characterization of HER2 Cell Receptor-Targeted Indocyanine Green-Encapsulated Poly (Lactic-co-Glycolic Acid) Nanoparticles

Abstract

Introduction: The aim of this study is to fabricate and characterize human epidermal growth factor receptor 2 (HER2)-targeted indocyanine green (ICG)-loaded poly (lactic-co-glycolic acid (PLGA) nanoparticles (HIPNPs).

Methods: The HIPNPs were fabricated by a modified emulsification in association with solvent evaporation approach. The size and surface charge of the manufactured nanoparticles were determined by dynamic light scattering technique. The morphology of the HIPNPs was detected by SEM. The activity of surface anchored anti-HER2 antibodies was detected by spectro fluorometry and fluorescent microscopy. The encapsulation rate of ICG, percentage of ICG content, and the degradation efficiencies of entrapped ICG under different temperatures were measured through UV-Vis spectrometry.

Results: All HIPNPs exhibited particulate morphology with size of 302 ± 1.8 nm and surface charge of -15 ± 0.15 mV where the polydispersity index was in the range of 0.02 - 0.07. The encapsulation rate of ICG and percentage of ICG content in the HIPNPs were 70% and 23%, respectively. The stability of ICG can be improved after encapsulated into the PLGA nanoparticles, by which the degradation rates of entrapped ICG in 4 °C and 37 °C aqueous medium significantly reduced about 6- and 3-fold, respectively, as compared to the freely dissolved ICG within 48 h.

Conclusions: We have successfully fabricated and characterized the HIPNPs in this study. Based on the enhanced stability, bioavailability, biocompatibility, and target-ability of the HIPNPs, the developed ICG Nano-carriers exhibited a high potential for use in near infrared-based diagnostics and therapeutics *in vitro* and/or *in vivo* for HER2-expressing cells.

Introduction

Indocyanine green (ICG), also known as cardio green, is an U.S. Food and Drug Administration-approved water-soluble tricarbocyanine dye that enables to absorb and fluoresce in the near-infrared (NIR) wavelength region (650 - 850 nm) [1]. As water and most intrinsic biomolecules in tissue do not absorb strongly within the NIR range [2], interest in using ICG as optical probe for deeper tissue structure is increasing. So far ICG has been extensively used and/or investigated in a variety of diagnostic applications including evaluation of cardiac output [3], NIR-Fluorescence image-guide surgery [4], lymph node detection in multiple types of cancers [5-7], and assessment of liver function [8]. In addition, since it can generate heat and singlet oxygen upon NIR irradiation, ICG has further motivated investigations into its utility on therapeutic purpose such as applications in photodynamic therapy, photo thermal therapy, and tissue welding [9-11].

However, currently the clinical efficacy of ICG remains limited by various factors including molecular instability, rapid circulation kinetics, and lack of target specificity. It has been reported that the degradation of ICG in aqueous medium follows first-order kinetics [12], and can be induced/accelerated by light exposure (photo-degradation) and/or heating (thermal-degradation) [12], leading to functionless of the ICG product since the degraded ICG molecules fail to fluoresce in NIR wavelength region [12]. Moreover, as being a fluorescence probe and/or photosensitizing agent for use *in vivo*, reagents are usually required to be equipped with properties of long circulation half-life, target-ability, and capability of accumulation at the disease site and/or prolong stay at the site of action. However, ICG administered intravenously can provide only about 2 - 4 min of plasmatic half-life and exhibit extensive protein binding in the duration of circulation [13,14]. Such circumstances seriously hampered the applicability of ICG and thus a strategy that enables to overcome the aforementioned drawbacks is certainly needed for development of ICG-based application.

Among various polymeric drug carriers, poly(lactic-co-glycolic acid) (PLGA) has been recognized as one of the most commonly used biomaterials with U.S. FDA approval for the encapsulation of therapeutics (e.g., ICG) due to its biocompatibility and biodegradability [15]. Furthermore, the degradation efficiency of

PLGA can be modulated by adjusting the molecular weight and/or ratio of lactide to glycolide in the PLGA molecules that renders a feature of controlled drug release to the drug carrier. Regarding the issue of drug carrier size, it has been known that the nanometer-sized particles enable to provide (1) improved bioavailability by enhancing aqueous solubility; (2) enhanced permeability on the target cells and (3) increasing retention time in the vasculature and/or tissue as compared to micro particles (d ≥ 1 μm). These features may result in decreased amount of payload required and therefore reduce dosage toxicity, offering an efficient delivery of therapeutics (e.g., ICG) with low side effects for non-targeted tissues and/or cells [16].

In this paper, we aimed to develop ICG-loaded PLGA nanoparticles with ligands-mediated target-ability for ICG delivery. The human epidermal growth factor receptor 2-targeted ICG-loaded PLGA nanoparticles (HIPNPs) were prepared by a modified emulsification in association with solvent evaporation approach, and the physicochemical properties of the resulting products including particle size, surface charge, morphology, activity of anchored ligands, encapsulation rate, percentage of ICG content, and the efficiency of ICG degradation *in vitro* were comprehensively investigated in this work.

Materials and Methods

Materials

Poly(lactic-co-glycolic acid) (PLGA; 50:50, MW = 7000 - 17000 kDa), polyvinyl alcohol (PVA), dichloromethane (DCM), 1-ethyl-3-(3-dimethylaminopropyl) carbodiimide hydrochloride (EDC), N-Hydroxysuccinimide (NHS), hetero-bifunctional polyethylene glycol (COOH-PEG-NH_2), and indocyanine green (ICG, absorption wavelength = 780 nm) were purchased from Sigma-Aldrich (St. Louis, MO). Anti-human epidermal growth factor receptor 2 monoclonal antibody (Anti-HER2-mAb) and Anti-mouse IgG secondary antibody were purchased from Cell Signaling (Danvers, MA). All chemicals were used as received.

Fabrication of HIPNPs

The HIPNPs were fabricated by a modified emulsification in association with solvent evaporation approach. Briefly, 30 mg of PLGA was first mixed with 1 mg of ICG in 1 mL DCM-methanol solution (v/v = 7:3). The mixture was then added to 15 mL of PVA solution (0.2 wt%) and emulsified by sonication at 100 W for 90 sec in an ice bath. The emulsified medium was then stirred for another 4 h at 700 rpm, followed by centrifugation at 20000 ×g for 20 min. The nanoparticles formed were then washed twice with PBS solution and re-suspended in 1-mL PBS. Afterward the collected nanoparticles were stepwise assembled with hetero-bifunctional PEG molecules and anti-HER2-mAb on the particle surface using EDC and NHS cross linkers to conjugate carboxyl and amide groups as reported previously [17]. The duplicate PBS washes were performed after completion of each time of crosslinking on the particle surface. Ultimately the HIPNPs were lyophilized for 48 h and stored at -20 °C until further use. The overall procedures of HIPNP manufacture was illustrated in Figure 1.

Characterization of HIPNPs

The mean size and surface charge of the HIPNPs after re-dissolved

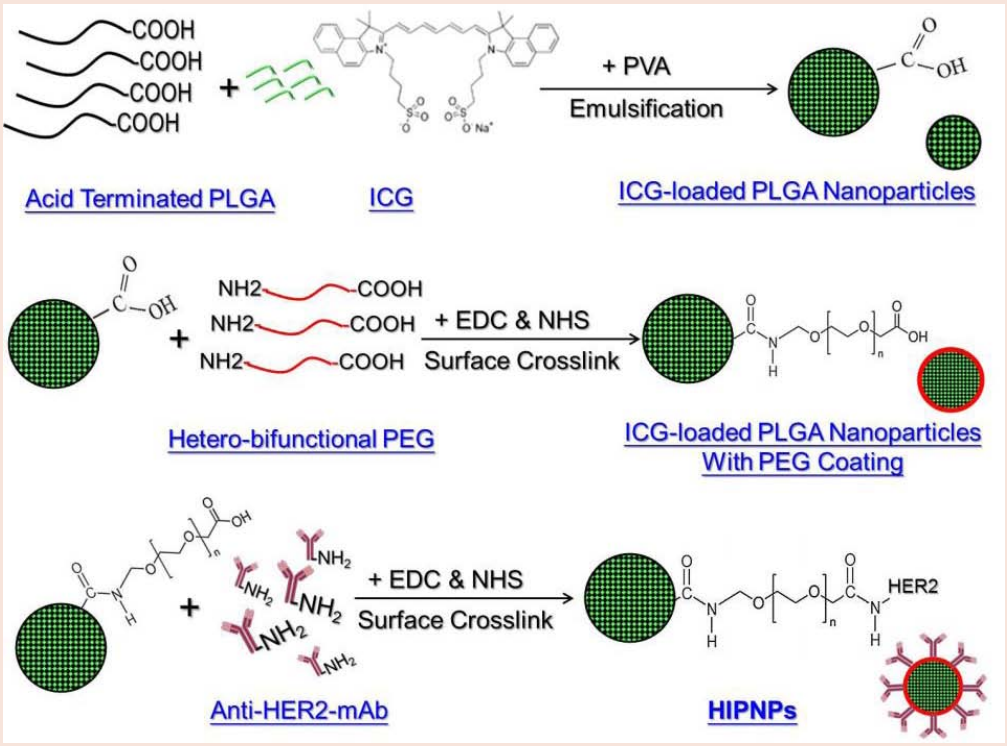

Figure 1: Schematic diagram illustrating the fabrication procedures of HIPNPs.

in deionized water (pH = 7) were measured using the dynamic light scattering (DLS; SZ-100 Particle Analyzer, HORIBA, Kyoto, Japan) technology. The morphology of the HIPNPs was detected by scanning electron microscopy (S-800 SEM; HITACHI, Tokyo, Japan) with an accelerating voltage of 20 kV. The encapsulation efficiency (E) of ICG in the HIPNPs was calculated by the formula:

$$E = \frac{W - W_I}{W} \times 100\% \quad (1)$$

Where W is the total amount of ICG used for fabrication of HIPNPs and W_I denotes the amount of free ICG molecules in the supernatant (i.e., un-encapsulated ICG) that was determined by Beer-Lambert's law. The percentage of ICG content in the HIPNPs (P) was calculated by the formula:

$$P = \frac{W_{ICG}}{W_H} \times 100\% \quad (2)$$

Where W_{ICG} is the mass of ICG encapsulated in the HIPNPs (i.e., $W \times E$) and W_H denotes the total weight of HIPNPs collected.

Efficiency of ICG degradation of HIPNPs

The effectiveness of ICG degradation for the HIPNPs was determined by monitoring the ICG amount remaining in the nanoparticles and comparing the degradation pattern performed by freely dissolved ICG (i.e., naked ICG molecules). Briefly, 6 mL of HIPNPs that were homogeneously distributed in the PBS was aliquoted into12 micro-centrifuge tubes. Six tubes were heated with 37 °C and the other six samples were maintained at 4 °C. All tubes were wrapped by foil to prevent ICG photo-degradation from light exposure. The ICG molecules remained in the HIPNPs in both temperature settings were detected in parallel at 0, 2, 4, 6, 24, and 48 h using UV–Vis spectrophotometry (V-650, JASCO, Easton, MD) at 780 nm, followed by quantification according to Beer-Lambert's law. The degradation rate (D) of ICG entrapped in the HIPNPs was calculated by the formula:

$$D = \left(1 - \frac{I_t}{I_0}\right) \times 100\% \quad (3)$$

Where I_t is the absorbance of HIPNPs detected at time t and I_0 denotes the initial absorbance of HIPNPs obtained before thermal stimulation.

Statistical analysis

All data were acquired from three independent experiments and are presented as mean ± standard deviation (SD). Statistical analyses were conducted by using MedCalc software in which comparisons for one condition between two groups were performed by Student's t-test with a significance level of $P < 0.05$ used throughout the study.

Results and Discussion

The photograph of HIPNP medium after washed twice with PBS was shown in Figure 2A (right), in which the green appearance of HIPNPs clearly demonstrated the existence of ICG in the particles as compared to the medium containing blank PLGA nanoparticles shown beside (Figure 2A, left). Figure 2B represents a three dimensional image of the HIPNP morphology obtained by SEM. Our data showed that the produced HIPNPs remained intact particulate shape without collapse after the fabrication procedures including high-speed centrifugation and long-time agitation.

According to the molecular structure as exhibited in Figure 1, ICG has two polycyclic parts and a sulfate group bound to each polycyclic group, offering both lipophilic and hydrophilic characters to the molecule. This amphiphilic nature enables the ICG molecules quickly partition out into the water from the organic phase during the emulsification and agitation processes that may adversely influence the efficacy of ICG encapsulation. In this study, the ICG encapsulation rate and percentage of ICG content in the HIPNPs were 70% and 23%, respectively, based on the calculations using Eq. (1) and Eq. (2) as mentioned above.

The sizes and surface charges of the PLGA nanoparticles with and without surface modifications (crosslinking with both PEG and anti-HER2-mAb) were detected as presented in Figure 3. Our data showed that the size and zeta potential of the nanoparticles

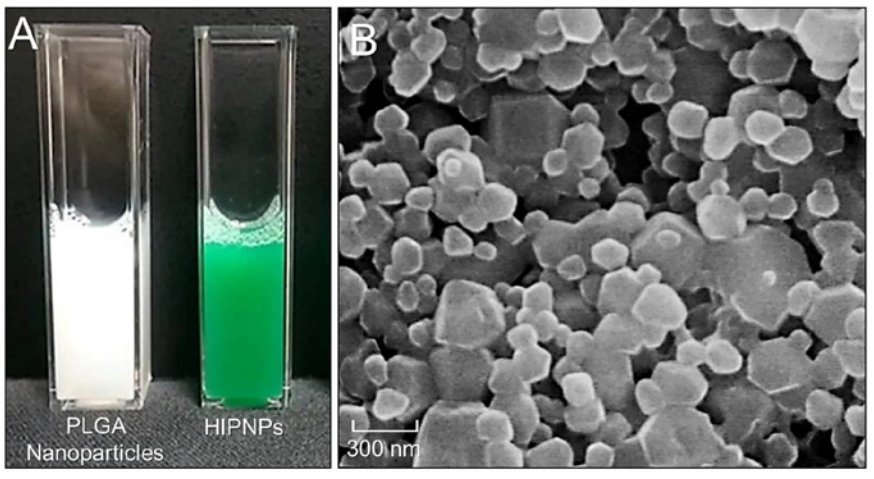

Figure 2: (A) Photographs of blank PLGA nanoparticle without payload (left) and HIPNP (right) media. (B) SEM image of HIPNPs. Scale bar = 300 nm.

post surface modifications increased and decreased about 74% and 60%, respectively, as compared to the bare ICG-loaded PLGA nanoparticles, resulting in a mean size of 302 ± 1.8 nm and surface charge of -15 ± 0.15 mV for the HIPNPs. It is understood that the particle size increased along with manufacture procedures because more molecules (PEG and antibodies) were congregated on the polymeric surface as illustrated in Figure 1. In terms of the decrease of surface charge, on the other hand, we reasoned that the factor which might be responsible for such an effect can be the presence of multi molecules including PEG and anti-HER2 antibodies on the nanoparticle surface. Generally, high negative zeta potential value is expected for pure nanoparticles made by polymer with acidic terminal (e.g., acid-terminated PLGA-made nanoparticles as shown in Figure 1) due to the presence of carboxyl groups on the polymeric chain extremities [18]. After conjugating with molecules, however, the additionally seeded molecules on the HIPNPs may create a shield between the nanoparticle surface and the surrounding medium to mask the possible charged groups existing on the particle surface, leading to reduction of zeta potential value as reported previously [18]. In addition, the polydispersity index (PI) of the HIPNPs was in the range of 0.02 - 0.07, indicating a narrow particle size distribution for the developed ICG carriers that can also be observed from the SEM image.

The presence and activity of anti-HER2 antibodies on the product surface was examined by conjugating bare ICG-loaded PLGA nanoparticles and HIPNPs with fluorescence-probed secondary antibodies separately and the results were shown in Figure 4. Our data showed that the group of HIPNP exhibited marked fluorescent expression (Figure 4, upper image B) while the sample without anti-HER2 antibody (i.e., ICG-loaded PLGA nanoparticles) was completely fluorescence negative (Figure 4, upper image A) that the level of fluorescence intensity was similar to the value obtained from water (blank control; P = NS). These results clearly manifested that the anti-HER2 antibodies were certainly bonded on the surface of nanoparticles after carboxyl-amide crosslinking procedures that conferred the HIPNPs a target-ability to HER2-positive cells accordingly.

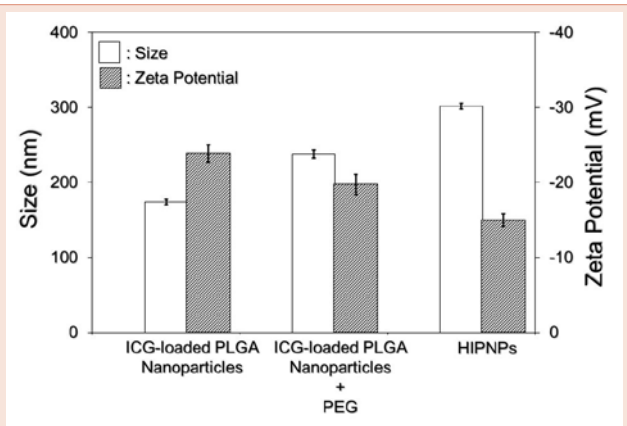

Figure 3: Quantitative analyses of the sizes (left Y-axis) and surface charges (right Y-axis) of the bare ICG-loaded PLGA nanoparticles, ICG-loaded PLGA nanoparticles coated with hetero-bifunctional PEG, and HIPNPs. Values are mean ± SD (n = 3).

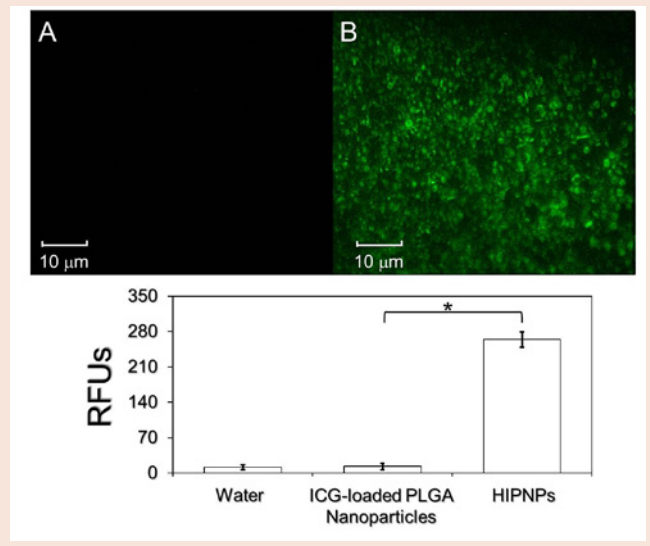

Figure 4: Verification of the presence and activity of anti-HER2 antibodies on the ICG-loaded PLGA nanoparticles. The upper panel exhibits fluoromicroscopic images of the ICG-loaded PLGA nanoparticles with neither PEG nor anti-HER2-mAb on the surface (A) and HIPNPs (B). Both types of the nanoparticles were treated with fluorescence-expressed anti-mouse IgG secondary antibodies and washed twice with PBS afterward. Scale bar = 10 μm. The bottom panel represents the quantitative analyses of the fluorescent intensities of the particles exhibited above that were measured by using spectrofluorometry with excitation wavelength of 490 nm and emission wavelength of 525 nm and quantitatively represented by relative fluorescence units (RFUs). The group of water was employed as the blank control. Values are mean ± SD (n = 3). *P < 0.05.

We subsequently analyzed the profile of ICG degradation in the HIPNPs. Since ICG degrades in aqueous medium and is very sensitive to light and thermal stimulations [12], it is not suitable to evaluate the degradation of ICG in the HIPNPs through detection of its concentration released in the supernatant (obtained by centrifugation) as performed in most of drug release investigations. In this study, the HIPNPs placed at 4 and 37 °C were directly subjected to UV-Vis spectrometry to determine the amount of ICG left in the nanoparticle matrix after 0 (without temperature stimulation), 2, 4, 6, 24, and 48-h exposure as utilized in the previous study [19], and the results were shown in Figure 5. We found that within 48-h incubation in dark, the degradation efficiencies of freely dissolved and HIPNPs-entrapped ICG molecules were 58.8% and 9.8%, respectively, at 4 °C; and were 95% and 36.8%, respectively, at 37 °C calculated based on Eq. (3), showing that the stability of entrapped ICG in 4 °C and 37 °C aqueous medium remarkably enhanced about 6- and 3-fold, respectively, as compared to the freely dissolved ICG within 48 h. These results indicated that the stability of ICG in aqueous medium can be remarkably improved while it was encapsulated into PLGA nanoparticles. Combined with enhanced bioavailability and biocompatibility contributed by the interlayer PEG molecules [20,21] and capability of cell targeting conferred by anchored anti-HER2 antibodies, the developed HIPNPs exhibited a high potential for ICG-related applications to HER2-overexpressing cells/tissues both *in vitro* and *in vivo*. However, further investigations are certainly required to identify the functionalities described above.

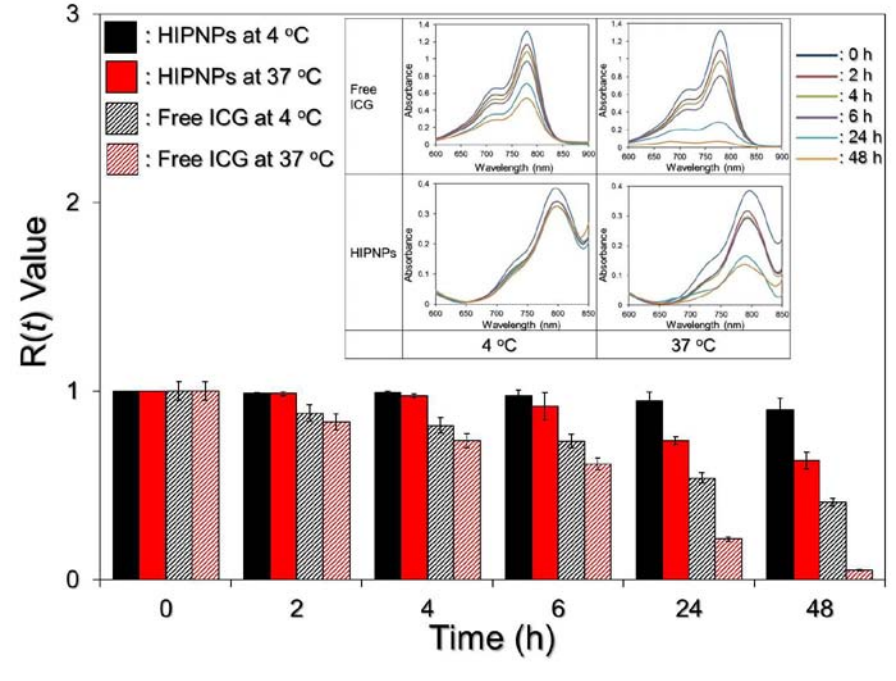

Figure 5: Influence of temperature on normalized peak absorbance of freely dissolved ICG and HIPNPs-protected ICG within 48 h. The initial concentrations of ICG in both groups were equalized to 100 μg/mL that were determined by using UV-Vis spectrometry. The inset curves represented the UV-Vis spectra of freely dissolved ICG and HIPNPs incubated under 4 and 37 oC for 48 h. R(t) = [abs (t, λ = 785 nm) / abs (t = 0, λ = 785 nm)] × 100%. Values are mean ± SD (n = 3).

Conclusion

In summary, we have presented the fabrication of ICG-loaded PLGA nanoparticles with HER2-targeting capacity (i.e., HIPNPs) using emulsification in association with solvent evaporation approach followed by surface modifications using hetero-bifunctional PEG molecules and anti-HER2 antibodies. The physicochemical characterizations of the HIPNPs, including the size, surface charge, morphology, encapsulation rate, percentage of ICG content, activity of cross linked anti-HER2 antibodies, and degradation efficiencies of entrapped ICG under different temperatures were comprehensively investigated. The results showed that the ICG can be encapsulated into PLGA matrix with considerable encapsulation rate, while the stability of encapsulated ICG can be tremendously enhanced as compared to freely dissolved ICG molecules in the aqueous medium. Further investigations by applying HIPNPs to NIR-based biomedical imaging operations and/or photo-therapeutic methodologies will be conducted to fully address the applicable value of the HIPNPs hypothesized, and efforts are currently in progress.

Acknowledgement

This work was financially supported by Ministry of Science and Technology in Taiwan, R.O.C. (MOST 104-2221-E-008-095; Y.-H. Lee).

References

1. Landsman ML, Kwant G, Mook GA, Zijlstra WG (1976) Light-absorbing properties, stability, and spectral stabilization of indocyanine green. J Appl Physiol 40: 575-583.
2. Welch AJ, van Gemert MJC, Star WM (2011) Definitions and Overview of Tissue Optics. New York: Springer−Verlag 15-46.
3. Jarrar D, Wang P, Song GY, Knöferl MW, Cioffi WG, et al. (2000) Metoclopramide: a novel adjunct for improving cardiac and hepatocellular functions after trauma-hemorrhage. Am J Physiol Endocrinol Metab 278: E90-E95.
4. Gibbs SL (2012) Near infrared fluorescence for image-guided surgery. Quant Imaging Med Surg 2: 177-187.
5. Abe H, Mori T, Umeda T, Tanaka M, Kawai Y, et al. (2011) Indocyanine green fluorescence imaging system for sentinel lymph node biopsies in early breast cancer patients. Surg Today 41: 197-202.
6. Fujiwara M, Mizukami T, Suzuki A, Fukamizu H (2009) Sentinel lymph node detection in skin cancer patients using real-time fluorescence navigation with indocyanine green: preliminary experience. J Plast Reconstr Aesthet Surg 62: e373-e378.
7. Tajima Y, Yamazaki K, Masuda Y, Kato M, Yasuda D, et al. (2009) Sentinel node mapping guided by indocyanine green fluorescence imaging in gastric cancer. Ann Surg 249: 58-62.
8. Halle BM, Poulsen TD, Pedersen HP (2014) Indocyanine green plasma disappearance rate as dynamic liver function test in critically ill patients. Acta Anaesthesiol Scand 58: 1214-1219.
9. Esposito G, Rossi F, Matteini P, Scerrati A, Puca A, et al. (2013) In vivo laser assisted microvascular repair and end-to-end anastomosis by means of indocyanine green-infused chitosan patches: a pilot study. Lasers Surg Med 45: 318-325.
10. Yanina IY, Tuchin VV, Navolokin NA, Matveeva OV, Bucharskaya AB, et al. (2012) Fat tissue histological study at indocyanine green-mediated photothermal/photodynamic treatment of the skin in vivo. J Biomed Opt 17: 058002.
11. Kuo WS, Chang YT, Cho KC, Chiu KC, Lien CH, et al. (2012) Gold nanomaterials conjugated with indocyanine green for dual-modality photodynamic and photothermal therapy. Biomaterials 33: 3270-3278.

12. Saxena V, Sadoqi M, Shao J (2003) Degradation kinetics of indocyanine green in aqueous solution. J Pharm Sci 92: 2090-2097.

13. Mordon S, Devoisselle JM, Soulie-Begu S, Desmettre T (1998) Indocyanine green: physicochemical factors affecting its fluorescence in vivo. Microvasc Res 55: 146-152.

14. Desmettre T, Devoisselle JM, Mordon S (2000) Fluorescence properties and metabolic features of indocyanine green (ICG) as related to angiography. Surv Ophthalmol 45: 15-27.

15. Shive MS, Anderson JM (1997) Biodegradation and biocompatibility of PLA and PLGA microspheres. Adv Drug Deliv Rev 28: 5-24.

16. Mudshinge SR, Deore AB, Patil S, Bhalgat CM (2011) Nanoparticles: Emerging carriers for drug delivery. Saudi Pharm J 19: 129-141.

17. Sehgal D, Vijay IK (1994) A method for the high efficiency of water-soluble carbodiimide-mediated amidation. Anal Biochem 218: 87-91.

18. Konan YN, Cerny R, Favet J, Berton M, Gurny R, et al. (2003) Preparation and characterization of sterile sub-200 nm meso-tetra(4-hydroxylphenyl) porphyrin-loaded nanoparticles for photodynamic therapy. Eur J Pharm Biopharm 55: 115-124.

19. Saxena V, Sadoqi M, Shao J (2004) Indocyanine green-loaded biodegradable nanoparticles: preparation, physicochemical characterization and in vitro release. Int J Pharm 278: 293-301.

20. Na HB, Palui G, Rosenberg JT, Ji X, Grant SC, et al. (2012) Multidentate catechol-based polyethylene glycol oligomers provide enhanced stability and biocompatibility to iron oxide nanoparticles. ACS Nano 6: 389-399.

21. Arun kumar R, Prashanth KV, Manabe Y, Hirata T, Sugawara T, et al. (2015) Biodegradable poly (lactic-co-glycolic acid)-polyethylene glycol nanocapsules: An efficient carrier for improved solubility, bioavailability, and anticancer property of lutein. J Pharm Sci 104: 2085-2093.

Citation: *Lee YH, Lai YH (2015) Fabrication and Characterization of HER2 Cell Receptor-Targeted Indocyanine Green-Encapsulated Poly (Lactic-co-Glycolic Acid) Nanoparticles. Peertechz J Biomed Eng 1(1): 015-020.*